

## Field-Induced Magnetic Transitions in the One-Dimensional Compound $\text{Ca}_3\text{Co}_2\text{O}_6$

Hiroshi KAGEYAMA\*, Kazuyoshi YOSHIMURA, Koji KOSUGE,  
Hiroyuki MITAMURA<sup>1</sup> and Tsuneaki GOTO<sup>1</sup>

*Department of Chemistry, Graduate School of Science, Kyoto University, Kyoto 606-01*

<sup>1</sup>*Institute for Solid State Physics, University of Tokyo, Roppongi, Tokyo 106*

(Received January 27, 1997)

Magnetization measurements on the one-dimensional oxide  $\text{Ca}_3\text{Co}_2\text{O}_6$  having a triangular net of  $\text{Co}_2\text{O}_6$  chains have been carried out both in static and pulsed high magnetic fields. The  $M/H$  vs.  $T$  curve obeys the Curie-Weiss law at high temperatures. Below 25 K, however,  $M/H$  increases abruptly, and a plateau is observed at 1/3 of the full moment in the  $M-H$  curve, suggesting a ferrimagnetic state of the ferromagnetic chains due to the antiferromagnetic interchain interaction. At low  $H$ , this system is considered to be in a partially disordered antiferromagnetic state for  $10 \text{ K} < T < 25 \text{ K}$  and in a ferrimagnetic state below 10 K. The observed plateau in the  $M-H$  curve for  $T \leq 5 \text{ K}$  is broader than for  $10 \text{ K} \leq T \leq 20 \text{ K}$ , indicating spin freezing at lower temperatures. The results can be discussed in terms of the triangular Ising spin systems.

**KEYWORDS:** ferrimagnetic transition, triangular lattice, frustration,  $\text{Ca}_3\text{Co}_2\text{O}_6$ , one-dimensional magnetic chain, Ising spin system, partially disordered antiferromagnetic phase

The cooperative phenomena associated with magnetic linear-chain systems are of great interest. Experimentally, many studies have been carried out on  $\text{CsCoCl}_3$ ,  $\text{RbFeCl}_3$  and other  $\text{ABO}_3$ -type compounds.<sup>1-5</sup> At low temperatures, these nearly one-dimensional systems exhibit transitions to a variety of three-dimensional ordered states. Such transition is induced by relatively weak coupling between chains of strongly coupled spins. The sign and magnitude of interchain and intrachain interactions are expected to determine the type of ordered state. Theoretically, the Ising spin model with antiferromagnetic nearest-neighbor interactions on the triangular lattice is investigated most extensively because of its simplicity. The unique magnetic properties of  $\text{CsCoCl}_3$  associated with the triangular lattice are known to be well explained by this model.<sup>6,7</sup>

Recently, Fjellvåg *et al.* have determined the crystal structure of  $\text{Ca}_3\text{Co}_2\text{O}_6$ ,<sup>8</sup> which is related to those of  $\text{Sr}_3\text{ABO}_6$  (where  $\text{A}=\text{Ni}, \text{Cu}, \text{Zn}, \text{B}=\text{Ir}, \text{Pt}$ ).<sup>9,10</sup>  $\text{Ca}_3\text{Co}_2\text{O}_6$  belongs to the space group  $R\bar{3}c$ . The structure of  $\text{Ca}_3\text{Co}_2\text{O}_6$  is shown in Fig. 1. Figure 1(a) shows the perspective view along the hexagonal [110] direction.  $\text{Sr}_3\text{ABO}_6$  consists of infinite chains of alternating face-sharing  $\text{AO}_6$  trigonal prisms and  $\text{BO}_6$  octahedra (antitrigonal prisms), whereas Co atoms occupy both A and B sites in  $\text{Ca}_3\text{Co}_2\text{O}_6$ . Consequently, the  $\text{Co}_2\text{O}_6$  infinite chains are built by successive alternating  $\text{CoO}_6$  trigonal prisms (with Co1) and  $\text{CoO}_6$  octahedra (with Co2) along the hexagonal  $c$ -axis. One-dimensional character along the  $c$ -axis can be expected because the  $\text{Co}_2\text{O}_6$  chains are widely spaced; the interchain separation is 5.24 Å which is about twice as large as the intrachain Co distance of

2.59 Å.<sup>8</sup>) Each  $\text{Co}_2\text{O}_6$  chain is surrounded by six chains forming a triangular net as shown in Fig. 1(b). Thus, we can expect cooperative phenomena caused by the triangular arrangement of the  $\text{Co}_2\text{O}_6$  chains. It should be noted that the phase of each chain is different from the phase of three nearest-neighbor chains by 1/6 along the  $c$ -axis (the chain direction) and from the phases of the other three by 2/6 along the same axis (see Fig. 1(a)).

To elucidate the magnetic behavior of  $\text{Ca}_3\text{Co}_2\text{O}_6$ , we have performed magnetization measurements at various temperatures under both static and pulsed fields up to 5 T and 40 T, respectively. The main finding is that the  $M-H$  curves below 25 K show stepwise magnetization; the first step is the ferrimagnetic plateau at 1/3 of the

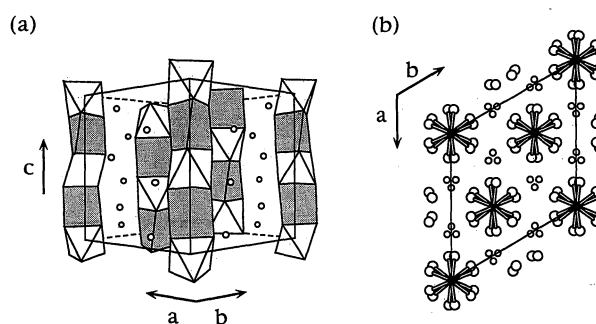


Fig. 1. Schematic illustration of the hexagonal structure of  $\text{Ca}_3\text{Co}_2\text{O}_6$ . (a) The perspective view along the [110] direction. The open and shaded polyhedra represent  $\text{CoO}_6$  octahedra (antitrigonal prisms) and  $\text{CoO}_6$  trigonal prisms, respectively. The open circles represent Ca atoms. (b) The projection along the  $c$ -axis. The black circles represent the cobalt, the large open circles the oxygen, and the small open circles the calcium atoms.

\* E-mail: kage@kuchem.kyoto-u.ac.jp

saturation magnetization and the second step over 10 T is full magnetization ( $1.8 \mu_B/\text{Co}$ ).

The  $\text{Ca}_3\text{Co}_2\text{O}_6$  sample was prepared by a solid state reaction method from  $\text{CaCO}_3$  and  $\text{CoO}$  with 99.99% purities. Powders were ground, pelletized and calcined in air at 1173 K for one day. Then, the sample was reheated at 1273 K in air for one week. Using the powder X-ray diffraction, the sample was confirmed to be in a single phase of  $\text{Ca}_3\text{Co}_2\text{O}_6$  with the space group  $R\bar{3}c$  and with the lattice parameters  $a=9.071 \text{ \AA}$  and  $c=10.375 \text{ \AA}$  in the hexagonal expression which was almost in agreement with the data of Fjellvåg *et al.*<sup>8)</sup> The magnetization was measured by using a SQUID magnetometer (Quantum Design MPMS) as a function of temperature ( $2 \text{ K} \leq T \leq 300 \text{ K}$ ) and field ( $0 \text{ T} \leq H \leq 5 \text{ T}$ ). The magnetic susceptibility  $\chi$  ( $=M/H$ ) for  $300 \text{ K} \leq T \leq 770 \text{ K}$  was measured at  $H=0.5 \text{ T}$  using a torsion magnetic balance. High field magnetization measurements were performed up to 40 T for powdered  $\text{Ca}_3\text{Co}_2\text{O}_6$  by an induction method with well balanced pick-up coils. The duration time of the pulsed magnetic field was 12 msec, corresponding to  $(\Delta H/\Delta t) = 6.7 \text{ T/msec}$ . We also performed magnetization measurements up to 6.2 T under the condition of  $(\Delta H/\Delta t) = 2.0 \text{ T/msec}$ .

First, we show, in Fig. 2, the temperature dependence of  $M/H$  measured using a SQUID magnetometer and a torsion magnetic balance. As seen in the inset of this figure,  $\chi$  is fitted well to the Curie-Weiss law over the range of 100 to 800 K with the Weiss temperature  $\theta=40.4 \text{ K}$  and the paramagnetic effective Bohr-magneton number  $P_{\text{eff}}=3.88 \mu_B/\text{Co}$ , accompanied with a constant susceptibility  $\chi_0=1.7 \times 10^{-4} \text{ emu/Co mol}$ . Below 100 K, the deviation from the Curie-Weiss law becomes appreciable. When the temperature is decreased to 25 K ( $=T_{c1}$ ), the values of  $M/H$  start to increase suddenly, and the magnetization curve shows non linear field dependence.

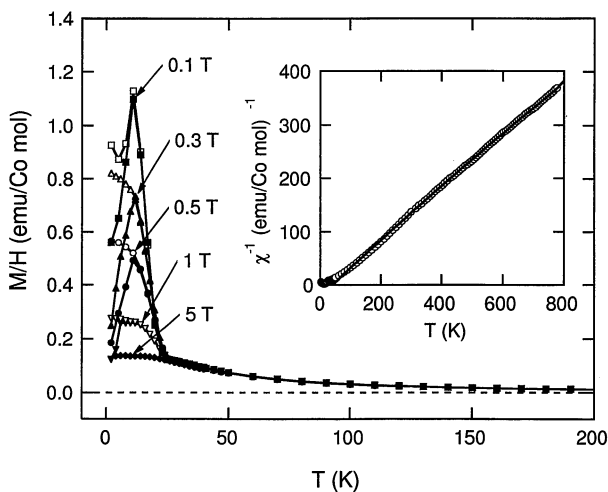


Fig. 2.  $M/H$  vs.  $T$  of  $\text{Ca}_3\text{Co}_2\text{O}_6$  under various static fields for  $2 \text{ K} \leq T \leq 200 \text{ K}$ . The open symbols represent the ZFC process and the solid symbols the FC process. Squares,  $H=0.1 \text{ T}$ ; triangles,  $0.3 \text{ T}$ ; circles,  $0.5 \text{ T}$ ; inverted triangles,  $1 \text{ T}$ ; diamonds,  $5 \text{ T}$ . The inset represents inverse magnetic susceptibility vs.  $T$  for  $2 \text{ K} \leq T \leq 770 \text{ K}$ . The solid line is the fit to the Curie-Weiss law, in which fitted parameters are written in the text.

A ferromagnetic intrachain interaction is deduced from the abrupt increase in the  $M/H$  vs.  $T$  curve and the positive value of  $\theta$ . The irreversibility in  $M/H$  vs.  $T$  curves appears at 10 K between zero-field-cooled (ZFC) and field-cooled (FC) processes.

Figure 3 shows the representative magnetization curves in static fields up to 5 T measured using a SQUID magnetometer. In the paramagnetic region above  $T_{c1}$ , the magnetization is proportional to  $H$ , as seen in the  $M-H$  curve at 30 K, whereas, below  $T_{c1}$ , non linearities appear in  $M-H$  curves. One can see a clear plateau in the  $M-H$  curves in the temperature range from 8 K to 16 K for  $H < 3 \text{ T}$  (see Fig. 3(a)), implying a ferrimagnetic ordering of ferromagnetic chains.

The magnetizations measured using pulsed fields are shown in Fig. 4. The magnetization at 35 K, where the spin system is in a paramagnetic state, is saturated toward  $1.8 \mu_B/\text{Co}$ . It should be noted that the  $M-H$  curve is almost temperature independent for  $H > 10 \text{ T}$ . This suggests that the magnetic transition at  $T_{c1}$  is not due to the change in the amplitude of Co moment which would be associated with a transition between the high spin state and the low spin one nor that of charge ordering between Co1 and Co2.

As seen in Fig. 4(b), one can observe a stepwise change in the magnetization at 15 K. The observed plateau is not clear and hysteresis is observed, in contrast to the  $M-H$  curve at 14 K in static fields. Hysteresis becomes clearer for  $T \leq 5 \text{ K}$  and will be discussed later. The plateau at 1/3 of the full moment strongly suggests a ferrimagnetic alignment of ferromagnetic chains. In the paramagnetic state, the short range ferromagnetic order develops predominantly along the magnetic chains. When the short range order is well developed as temperature

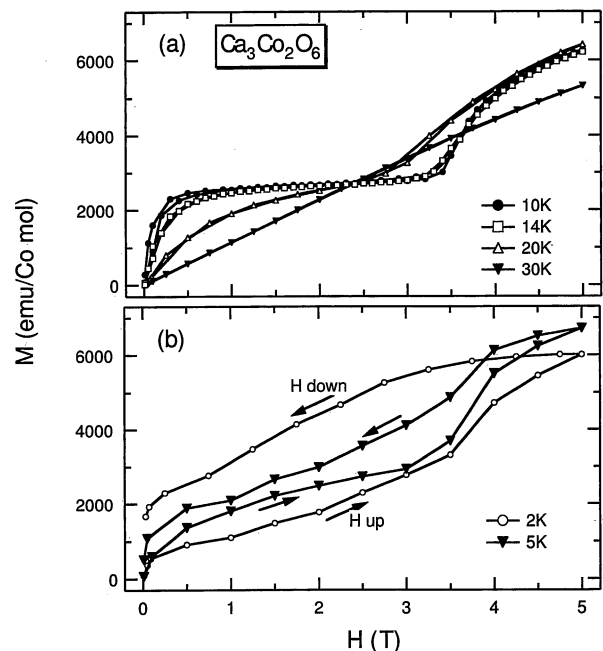


Fig. 3. Magnetization curves of  $\text{Ca}_3\text{Co}_2\text{O}_6$  in a static magnetic field for  $0 \text{ K} \leq H \leq 5 \text{ T}$  at 10, 14, 20 and 30 K (a), and 2 and 5 K (b). The arrows along the curves indicate the directions of the field sweep.

decreases, each ferromagnetic chain would behave like a magnetic moment. Therefore, the resultant magnetic structure should have two-dimensional character, resulting in a triangular-lattice antiferromagnet. The ferrimagnetic state indicates an antiferromagnetic interchain interaction. In the triangular lattice Heisenberg spin system, a  $120^\circ$  structure, where spins rotate successively by  $120^\circ$ , is stable.<sup>7)</sup> Therefore, Co spins would have Ising-like character. The molecular field theory for an antiferromagnetic triangular Ising lattice gives phase transition from a paramagnetic to a ferrimagnetic state.<sup>6)</sup>

Some compounds with a triangular net have been reported to exhibit ferrimagnetic ordering. In the case of  $\text{NaNi acac}_3\cdot\text{benzene}$ , however, there is no one-dimensional chain.<sup>11,12)</sup> As for  $\text{Ca}_3\text{Co}_2\text{O}_6$ , the ground state is a  $120^\circ$  state and a ferrimagnetic state is induced by a field, which is explained by an energy crossing between these two states.<sup>13)</sup> In the case of  $\text{CsCoCl}_3$ , intrachain interaction is antiferromagnetic, in contrast to  $\text{Ca}_3\text{Co}_2\text{O}_6$ .<sup>2,5)</sup> To the authors' knowledge, this is the first observation of the ferrimagnetic ordering of well-developed ferromagnetic chains among triangular lattice systems.

From the Arrott plots for the magnetization data in static fields,  $\text{Ca}_3\text{Co}_2\text{O}_6$  is in a ferrimagnetic state below  $T_{c2}=10$  K at zero field. Therefore, the observed metamagnetic transition below 10 K is from a ferrimagnetic to a ferromagnetic state. For  $T_{c2} < T < T_{c1}$ , on the other hand, a partially disordered antiferromagnetic (PDA) phase is possible in low fields, in which 2/3 of the chains exhibit antiferromagnetic order, leaving the re-

maining 1/3 incoherent with respect to the other chains. According to ref. 6, a PDA phase between a paramagnetic and a ferrimagnetic states is predicted at zero magnetic field. From neutron diffraction measurements at  $T=12$  K ( $> T_{c2}$ ) and under zero magnetic field, we successfully observed magnetic reflections, which are likely to be those from the PDA phase.<sup>14)</sup> In a PDA state only incoherent chains would contribute to the increase in magnetization as seen in the  $M$ - $H$  curve at 15 K. Since the propagation of a domain wall in the ferromagnetic chain is considered to be more difficult than in the case of the antiferromagnetic chain,<sup>15,16)</sup> thermal fluctuations and the interaction between two or three solitons may be important for facilitating the soliton motion in the ferromagnetic chain. Further study is needed in order to confirm the existence of the PDA phase.

Finally, let us discuss the magnetic behavior for  $T \leq 10$  K. As seen in Fig. 3(b), prominent hysteresis is observed and the metamagnetic transition is broadened, compared with that for  $T \geq 10$  K. The hysteresis at 2 K is much larger than that at 5 K. As mentioned above, the  $M/H$  vs.  $T$  curve shows a spin freezing below 10 K; the irreversibility between  $(M/H)_{\text{ZFC}}$  and  $(M/H)_{\text{FC}}$  was observed around 10 K. In the case of a pulsed field with  $(\Delta H/\Delta t) = 6.7$  T/msec, on the other hand, the magnetization at 4 K is completely different from that obtained in the static field measurements (*cf.* Fig. 3(b) and Fig. 4(c)). In the case of  $(\Delta H/\Delta t) = 2.0$  T/msec, a plateau in the  $M$ - $H$  curves was observed, as shown in the inset of Figs. 4(b) and 4(c). This result indicates that the ferromagnetic chains (or Co spins) respond to an external field at a rate of the order of  $10^{-3}$  sec. For  $\text{NaNi acac}_3\cdot\text{benzene}$ , similar behavior is observed under the condition of  $(\Delta H/\Delta t)=300$  T/msec, which is explained as the energy level crossing of the  $d$ -orbitals of  $\text{Ni}^{2+}$ .<sup>13)</sup> However, the energy level crossing is not likely to occur for  $\text{Ca}_3\text{Co}_2\text{O}_6$  because the field sweeping rate is much smaller than that in the case of ref. 13. We cannot give a reasonable explanation for the change from the ferrimagnetic to the spin freezing phase. The difference in the configuration of nearest-neighbor chains and/or an interchain interaction between separated chains such as the third and fourth nearest-neighbor chains may play a part.

In summary, we propose a rough magnetic phase diagram of  $\text{Ca}_3\text{Co}_2\text{O}_6$ , as shown in Fig. 5.

Although we have clarified the magnetic properties of  $\text{Ca}_3\text{Co}_2\text{O}_6$  in terms of the one-dimensional ferromagnetic chain, the moment of each cobalt ion is not clear. Since there are two different Co sites, two possibilities can be considered regarding the Co valence: (1) Co ions at both sites are trivalent. (2) one Co ion is divalent and the other tetravalent. It is also unknown whether Co spins are in the low spin state or the high spin state in connection with the energy level splitting of  $d$ -orbitals by the crystalline field of an octahedron and a trigonal prism. Furthermore, assuming that the  $g$  factor is 2, the saturation moment corresponds to about two thirds of the value expected from the experimental  $P_{\text{eff}}=3.88 \mu_B/\text{Co}$ . This small value should be interpreted using the fictitious spin  $S'$  of  $\text{Co}^{2+}$  ions as in the case of Ising spin

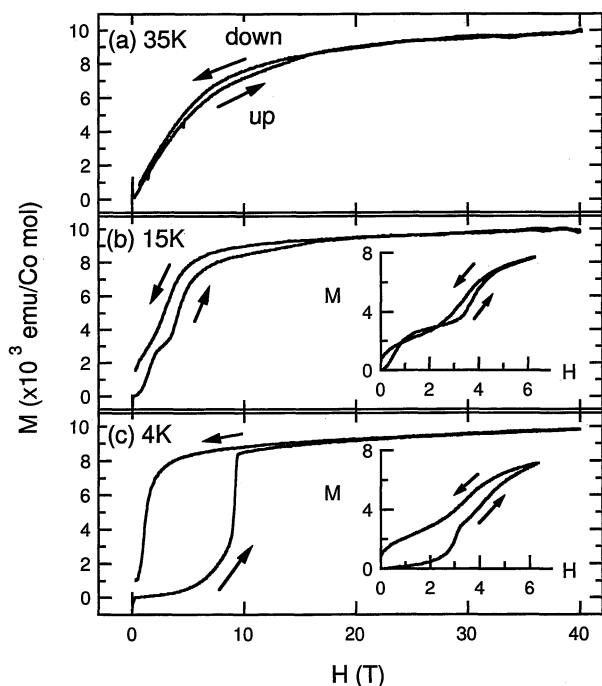


Fig. 4. Magnetization curves of  $\text{Ca}_3\text{Co}_2\text{O}_6$  under high pulsed magnetic fields up to 40 T with  $(\Delta H/\Delta t) = 6.7$  T/msec at 35 K (a), 15 K (b), and 4 K (c). The arrows along the curves indicate the directions of the field sweep. The inset represents magnetization curves up to 6.2 T with  $(\Delta H/\Delta t) = 2.0$  T/msec at 15 K (b) and 4 K (c) plotted in the same units as the main plot.

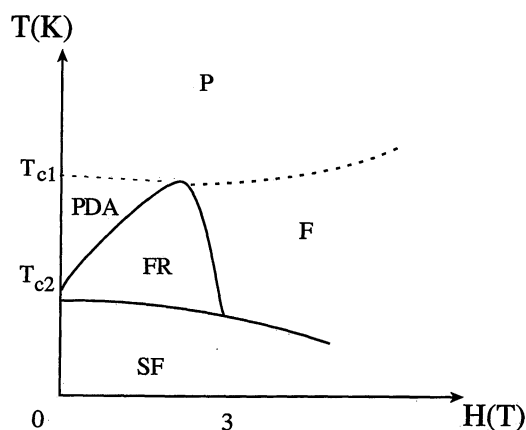


Fig. 5. Schematic phase diagram as a function of  $H$  and  $T$ . FR, a ferrimagnetic state; F, a ferromagnetic state; SF, a spin freezing state; P, a paramagnetic state; PDA, a partially disordered antiferromagnetic state.

systems.<sup>5,17)</sup>

For the further understanding of the magnetic properties of  $\text{Ca}_3\text{Co}_2\text{O}_6$ , specific heat, neutron diffraction, NMR and ESR measurements are now in progress. A single crystal will be required although all attempts have been unsuccessful to date.

In conclusion, we have measured magnetization up to 40 T for  $\text{Ca}_3\text{Co}_2\text{O}_6$  and observed a plateau at  $1/3$  of the full moment. This indicates ferrimagnetic alignment between the ferromagnetic chains, due to the antiferro-

magnetic interaction between ferromagnetic chains on a triangular lattice. Ferrimagnetic transition temperature  $T_{c2}$  at zero field is 10 K. A spin freezing behavior is observed at lower temperatures. A PDA state is possibly realized for  $T_{c2} < T < T_{c1}$ .

- 1) Y. Ajiro, H. Kikuchi, T. Okita, M. Chiba, K. Adachi, M. Mekata and T. Goto: J. Phys. Soc. Jpn. **58** (1989) 390.
- 2) M. Mekata and K. Adachi: J. Phys. Soc. Jpn. **44** (1978) 806.
- 3) K. Adachi: J. Phys. Soc. Jpn. **50** (1981) 3904.
- 4) M. Eibschütz, M. E. Lines and R. C. Sherwood: Phys. Rev. B **11** (1975) 4595.
- 5) N. Achiwa: J. Phys. Soc. Jpn. **27** (1969) 561.
- 6) M. Mekata: J. Phys. Soc. Jpn. **42** (1977) 76.
- 7) S. Miyashita: J. Phys. Soc. Jpn. **55** (1986) 3605.
- 8) H. Fjellvåg, E. Gulbrandsen, S. Aasland, A. Olsen and B. C. Hauback: J. Solid State Chem. **124** (1996) 190.
- 9) T. N. Nguyen, D. M. Giaquinta and H. C. zur Loye: Chem. of Mater **6** (1994) 1642.
- 10) T. N. Nguyen and H. C. zur Loye: J. Solid State Chem. **117** (1995) 300.
- 11) N. Yamada, Y. Karaki, N. Wada and K. Amaya: J. Phys. Soc. Jpn. **50** (1989) 3911.
- 12) K. Amaya, N. Yamada, Y. Karaki, N. Wada and T. Haseda: Physica **108B** (1981) 839.
- 13) T. Sakakibara and M. Date: J. Solid State Chem. **53** (1984) 3599.
- 14) H. Kageyama, S. Kawano, K. Yoshimura and K. Kosuge: in preparation
- 15) J. Villain: Physica **79B** (1975) 1.
- 16) H. C. Fogedby: Phys. Rev. B **8** (1973) 2200.
- 17) M. E. Lines: Phys. Rev. **131** (1963) 546.